NaAlSi: a self-doped semimetallic superconductor with free electrons and covalent holes

H. B. Rhee, S. Banerjee, E. R. Ylvisaker, and W. E. Pickett
Department of Physics, University of California, Davis, CA 95616
(Dated: December 31, 2009)

The layered ternary *sp* conductor NaAlSi, possessing the iron-pnictide "111" crystal structure, superconducts at 7 K. Using density functional methods, we show that this compound is an intrinsic (self-doped) low-carrier-density semimetal with a number of unusual features. Covalent Al-Si valence bands provide the holes, and free-electron-like Al 3*s* bands, which propagate in the channel between the neighboring Si layers, dip just below the Fermi level to create the electron carriers. The Fermi level (and therefore the superconducting carriers) lies in a narrow and sharp peak within a pseudogap in the density of states. The small peak arises from valence bands which are nearly of pure Si, quasi-two-dimensional, flat, and coupled to Al conduction bands. Isostructural NaAlGe, which is not superconducting above 1.6 K, has almost exactly the same band structure except for one missing piece of small Fermi surface. Certain deformation potentials induced by Si and Na displacements along the *c*-axis are calculated and discussed. It seems likely that the mechanism of pairing is related to that of several other lightly doped two-dimensional nonmagnetic semiconductors (TiNCl, ZrNCl, HfNCl), which is not well understood but apparently not of phonon origin.

PACS numbers:

I. INTRODUCTION

The discovery of new superconductors in unexpected materials brings the potential to understand something deeper, or perhaps something different, about the underlying properties that favor superconducting pairing. The discovery of high-temperature superconductivity (to 56 K so far) in Fe-pnictides[1] is a recent spectacular example, and is also an example of close relationships between magnetism and superconductivity, though the connections are still far from clear.

New superconductors where little or no magnetic effects are present are also arising, and these clearly involve different physics from the cuprate or Fe-pnictide high-temperature superconductors. Electron-doped MNCl, where M = Zr or Hf, becomes superconducting immediately upon undergoing the insulator-to-metal transition,[2–5] which, in the case of M = Hf, is higher than 25 K. The similarly layered, electron-doped, ionic insulator TiNCl superconducts up to 16 K. Magnetic behavior in these materials is at most subtle, amounting to an enhancement in Pauli susceptibility near the metal-to-insulator transition.[6]

In this paper we address the ternary silicide NaAlSi (space group *P4/nmm*, $Z = 2$), another ionic and layered material that shows unexpected superconductivity, and does so in its native (without doping or pressure) stoichiometric state, at 7 K.[7] NaAlSi introduces new interest from several viewpoints. First, it is an *sp* electron superconductor, with a high T_c for such materials at ambient pressure. Pb is an *sp* superconductor with comparable T_c (7.2 K) but with simple metallic bonding and heavy atoms, making it very different. Doped Si[8] and doped diamond[11] superconduct in the same range, and are of course very different classes of materials. A more relevant example is the pseudo-ternary compound $Ba_{1-x}K_xBiO_3$ (BKBO), which undergoes an insulator-to-metal transition for $x \approx 0.4$, beyond which its T_c surpasses 30 K.[9,10]

Second, the Al-Si layered substructure is like that of the FeAs layer in the Fe-pnictide superconductors, raising the possibility of some connections between their electronic structures. In fact, NaAlSi has the same structure as the Fe-pnictide "111" compounds, with Al being tetrahedrally coordinated by Si (analogous to Fe being tetrahedrally coordinated by As). In spite of their structural similarities, these compounds have major differences; for example, the Fe pnictides are 3*d* electron systems with magnetism, while NaAlSi is an *sp* electron system without magnetism.

Third, NaAlSi is the isovalent sister (one row down in the periodic table for each atom) of LiBC. LiBC itself is (in a sense) isovalent and also isostructural to MgB_2; however due to the B-C alternation around the hexagon in the honeycomb-structure layer, LiBC is insulating rather than conducting. When hole-doped while retaining the same structure, $Li_{1-x}BC$ has stronger electron-phonon coupling than does MgB_2.[12] While NaAlSi has a substantially different structure than LiBC, its isovalence and its combination of covalence with some ionic character is shared with LiBC.

Yet another closely related compound is CaAlSi, whose two different stacking polymorphs and parent structure superconduct in the 5–8 K range.[13,14] Linear-response and frozen-mode calculations indicate electron-phonon coupling is the likely mech-

anism; in particular, an ultra-soft phonon mode appears and is suggested to play a role in the superconductivity.[15–20] It is curious that in this compound, where divalent Ca (comparing it with NaAlSi) contributes one additional electron into the Si-Al *sp* bands, the preferred structure is that of AlB_2 (*i.e.*, MgB_2) with sp^2 planar bonding[15,16,18] rather than the more sp^3-like bonding in NaAlSi. Electronic structure calculations show that CaAlSi has one electron in the conduction band above a bonding-antibonding band separation at the NaAlSi band-filling level, a situation which would not appear to be particularly favorable for sp^2 bonding.

In this paper we analyze first-principles electronic structure calculations that reveal that NaAlSi is a naturally self-doped semimetal, with doping occurring—thus charge transfer occurring—between covalent bands within the Al-Si substructure, and two-dimensional (2D) free-electron-like bands within the Al layer. The resulting small Fermi surfaces (FSs) are unusual, complicated by the small but seemingly important interlayer coupling along the crystalline *c*-axis.

II. COMPUTATIONAL METHODS

First-principles, local density approximation (LDA) calculations were carried out using the full-potential local-orbital (FPLO) scheme.[21] A k-point mesh of $20\times20\times12$ was used, and the Perdew-Wang 92 approximation[22] was applied for the exchange-correlation potential. The experimental lattice constants obtained by Kuroiwa *et al.*[7] (a = 4.119 Å and c = 7.632 Å) and internal coordinates published by Westerhaus and Schuster[23] (z_{Na} = 0.622, z_{Si} = 0.223) were used in our calculations.

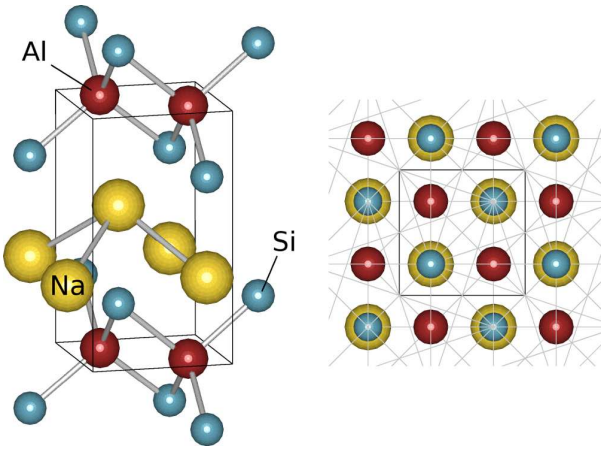

FIG. 1: (Color online.) Crystal structure[24] of NaAlSi. Four Si atoms tetrahedrally surround an Al atom, and these Al-Si networks sandwich the Na atoms. The unit cell is outlined in black.

III. ELECTRONIC STRUCTURE

A. Discussion of the band structure

The calculated band structure of NaAlSi is shown in Fig. 2. As expected, the Na ion gives up its electron to the Si-Al-Si trilayer (see Fig. 1), which may have some ionic character, though it is not easy to quantify (the valence bands have much more Si character than Al character, seemingly more than suggested by their number of valence electrons). There are several readily identifiable classes of bands. Two primarily Si 3*s* bands, with a small amount of Al 3*s* character, are centered 9 eV below the Fermi level ε_F and have a width of 2.5 eV. Above them there is a six-band complex of Al-Si *s*-*p* bands (heavily Si) that are very nearly filled, the band maximum only slightly overlapping ε_F.

Above ε_F lie non-bonding and antibonding bands, and the Na *s* bands. Among these there are a pair of distinctive bands, which can be identified most easily by their Al *s* character in the top panel of Fig. 2. These bands are nearly free-electron-like with large dispersions, and cross many other bands with little mixing. Along Γ-M they are degenerate and easily identifiable in Fig. 2, as they disperse up through the Fermi level to nearly 10 eV at the M point. Along Γ-X, and similarly at the top of the zone Z-R, they are distinct: one again disperses upward rapidly, cutting through many other bands, also to nearly 10 eV at X; the other disperses much more weakly to X, with a bandwidth of about 2 eV. Their Al *s* character and nearly vanishing Si character identify these as free-electron states, in which electrons move down channels of Al atoms separately in x and y directions. (Note that their lack of k_z dispersion identifies them as planar bands.) There is some coupling to the states in a parallel channel of Al atoms, giving rise to the 2 eV transverse dispersion. These bands lie 0.5 eV below ε_F at Γ and contain electrons. Without interference with other bands near the Fermi level and supposing them to be isotropic in the plane (but see below), such FSs might include 3–4% of the area of the zone, which would equate to an intrinsic electron doping for two bands, both spins of around 0.12–0.16 carriers per unit cell, and the concentration of hole carriers would be equal. The anisotropy, discussed below, makes the actual carrier concentration much lower.

The small overlap of valence and conduction bands results in semimetallic character and small Fermi surfaces. The valence bands are quite anisotropic. Looking at the valence bands along

Γ-X, one might try to characterize them as one "heavy-hole" and one "light-hole" band, degenerate at Γ, with the band maximum lying 0.13 eV above ε_F. However, the heavy hole band is actually almost perfectly flat for the first third of the Γ-X line, before dispersing downward across ε_F and farther below. Due to this flatness, the band cannot be characterized by an effective mass. The conduction bands contribute the pair of light electron bands described above. In addition, one conduction band dips slightly below the Fermi level along Γ-M near M.

The fatbands representation in Fig. 2 that reveals the dominant band character shows that the Si $3p_x$, $3p_y$, and Al $3s$ orbitals dominate the valence states near ε_F. As anticipated from consideration of the layered structure as mentioned earlier, the electronic structure is quasi-2D, with generally small dispersion along k_z near ε_F. However, the small k_z dispersion of one band is important in determining the geometry of the FSs, as discussed in more detail below.

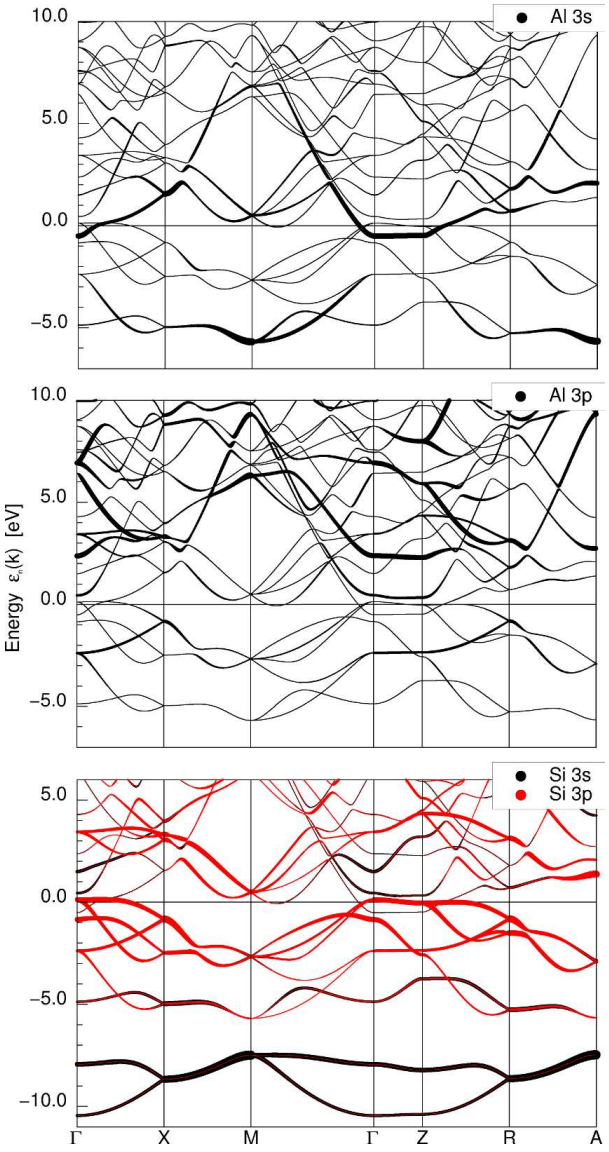

FIG. 2: (Color online.) Band structure, with projected fatbands, of NaAlSi. Top panel: the Al $3s$ character of bands is indicated by broadening. A doubly degenerate pair of broad bands is evident along the Γ-M direction. Middle panel: Al $3p$ character is weak below 2–3 eV. Bottom panel: Si $3s$ (black) bands below −8 eV, and Si $3p$ in the valence bands and lower conduction bands.

B. Density of states

Fig. 3 shows the total, partial, and projected densities of states (DOS) of NaAlSi. The Na contribution near the Fermi level is negligible and thus

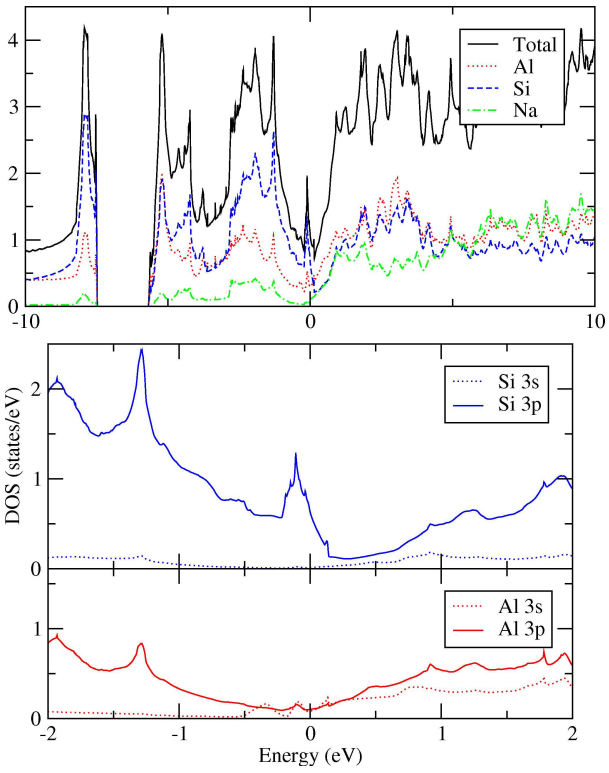

FIG. 3: (Color online.) Total and partial (atom- and orbital-projected) DOSs of NaAlSi. Top panel: Total and atom-projected DOS in a 20 eV-wide region, showing the pseudogap centered at the Fermi level (the zero of energy) punctuated by the curiously narrow and sharp peak at the Fermi level. Middle panel: expanded view of the peak, and the variation of the DOS near the Fermi level, separated into Si s and p contributions. Lower panel: the Al s and p character; the s character "turns on" just below the Fermi level.

not shown. Except for a strong dip ("pseudogap") near the Fermi level and a less severe dip in the −3 to −4 eV range, the DOS hovers around 3 states/eV throughout both valence and conduction bands. Within the pseudogap encompassing the Fermi energy, there is an anomalous sharp and narrow peak with ε_F lying on its upper slope, as noted previously by Kuroiwa *et al.*[7] The value of $N(\varepsilon_F)$ is 1.1 states/eV. We discuss below the FSs of both hole (Si) and electron (Al) character.

It seems clear that the transport properties and low-energy properties (which have not yet been reported), and in particular the superconductivity of NaAlSi, are intimately associated with this sharp and narrow peak in the DOS, which includes the Fermi level. The projected DOS shows the flat bands that give rise to this peak are very strongly Si-derived. There is Al 3*s* character that turns on just below ε_F, but it is relatively small compared to the Si character at ε_F, and its magnitude remains low and nearly constant through the peak. There is Al 3*p* character of the same magnitude in the vicinity of the Fermi level. The top edge of the peak coincides with the flat band along Γ-X at 0.13 eV. The width of the peak, about 0.35 eV, must be due to dispersion and anticrossings that are mostly not visible along symmetry directions and arise from mixing away from symmetry lines of the valence and conduction bands.

Nonetheless, the slope of the DOS at ε_F is rather steep, and this may give rise to high thermopower for the material. The standard low-temperature limit of thermopower (the Seebeck coefficient tensor) $\mathbf{S}(T)$ in semiclassical Bloch-Boltzmann theory is

$$\mathbf{S}(T) \to -\frac{\pi^2 k_B}{3e} \left. \frac{d \ln \boldsymbol{\sigma}(E)}{dE} \right|_{\varepsilon_F} k_B T. \qquad (1)$$

The conductivity tensor $\boldsymbol{\sigma}(E)$ can be written in terms of the average velocity ($\vec{v}(E)$) product, DOS, and scattering time $\tau(E)$ over the constant energy (E) surface:

$$\boldsymbol{\sigma}(E) = 4\pi e^2 \langle \vec{v}(E)\vec{v}(E) \rangle N(E)\tau(E). \qquad (2)$$

The thermopower thus picks up contributions from the energy variation of three quantities: the dyadic product $\langle \vec{v}\vec{v} \rangle$, $N(E)$, and $\tau(E)$. Often the energy dependence of τ is neglected, out of lack of detailed knowledge, though it also can be argued to follow roughly $1/\tau(E) \propto N(E)$ for elastic scattering. The energy dependence of $v^2(E)$ also counteracts the energy dependence of $N(E)$. Nevertheless it is observed that materials with large slope in $N(E)$ frequently have large thermopower. For NaAlSi we calculate $d \ln N(E)/dE|_{\varepsilon_F} = -4.0$ eV^{-1}. This value can be compared with other materials that have fine structure near the Fermi level: $TiBe_2$, where $d \ln N(E)/dE|_{\varepsilon_F} = 10$–$12$ eV^{-1} and $N(\varepsilon_F)$ also is much larger;[25] and $MgCNi_3$ with its very impressive peak very near ε_F, for which $d \ln N(E)/dE|_{\varepsilon_F}$ $\sim$ -15-20/eV^{-1}.[26]

The energy derivative of diagonal elements of $\boldsymbol{\sigma}$ that occurs in Eq. 1 can also be expressed as

$$\frac{1}{\sigma}\frac{d\sigma}{dE} = \frac{d \ln \tau(E)}{dE} + \frac{1}{2\pi^2}\frac{\mathcal{M}^{-1}(E)}{v^2(E)}, \qquad (3)$$

where $\mathcal{M}^{-1}(E)$ is (a diagonal element of) the inverse mass tensor (second derivative of ε_k) averaged over the constant energy surface. This form makes it clear that the expressions should, for any quantitative estimate, be generalized to two-band form, since the valence and conduction bands have differing signs of their effective masses, and the scattering time—and its energy variation—is likely to be very different for Si-derived covalent valence bands and Al-derived free-electron conduction bands. Measurement of the thermopower, and a quantitative theoretical treatment, would be very useful in extending the understanding of the transport properties of NaAlSi.

C. Unusual Fermi surfaces

Fig. 4 depicts the calculated FSs. In spite of the generally 2D band structure, the small k_z dispersion

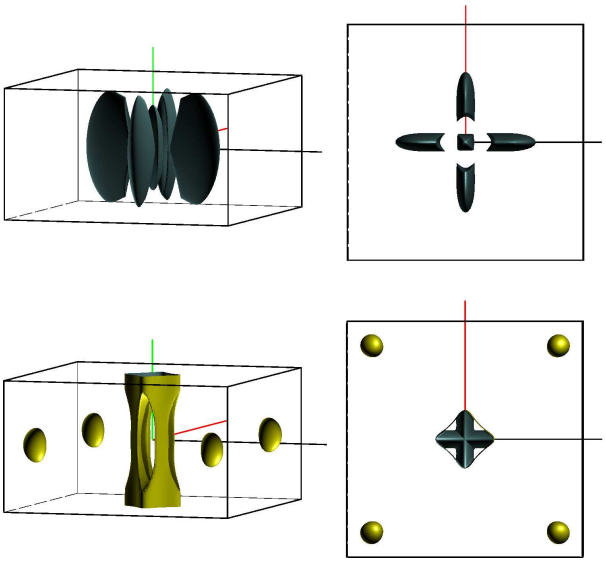

FIG. 4: (Color online.) Views from the xy-plane (left) and top (right) of the FSs of NaAlSi, centered at Γ. The blue (dark) surfaces enclose holes and the yellow (light) surfaces enclose electrons.

of bands at ε_F make some of the FSs surprisingly three-dimensional. Electron pockets and hole pockets coexist in the Brillouin zone, with electron and hole concentrations necessarily being equal.

Hole surfaces. Four hole "fan-blade" surfaces lie oriented in the xz- and yz-planes. At the center, extending from Γ half way to Z, lies a long and narrow surface with square cross section. The top view allows the origin of these surfaces to be understood. The cross sections in the xy-plane are of two ellipses that are very anisotropic (in the xy-plane) and at right angels to each other. Each corresponds to a dispersion that is weak in one direction (the long major axis) and strong in the other (minor axis). These bands would intersect, but in fact are intersected by the electron band that cuts a squarish hole (rotated by 45°), within which the elongated hole surface inside re-emerges.

Electron surfaces. In the bottom panels of Fig. 4, the squarish electron surface (with k_z variation and resulting holes, shown in the lower two panels of Fig. 4) that cuts the aforementioned hole surface is pictured, and substantiates the discussion provided just above. In addition, there are simple electron ellipsoids centered along the Γ-M lines. It is curious that in a band structure that is for the most part strongly 2D, all the FSs have a rather definite three-dimensional character. Although the bands show little dispersion along Γ-Z, the bands just above the the Fermi level are quite different depending on whether $k_z = 0$ or $k_z = \pi$. In particular, the lowest band along R-A is rather flat, but the lowest conduction band along X-M has a dispersion of nearly 2 eV. Similar comparisons can be made for the bands along Γ-X and Z-R. The k_z dispersion is not nearly as strong near $k_x = k_y = 0$, which is clear from both the band structure and the FS.

Short discussion. It was noted in the Introduction that the NaAlSi structure is the same as the Fe-pnictide "111" structure. Moreover, in both compounds, the relevant bands involve only the (Si-Al-Si or As-Fe-As) trilayer. The top view of the fan-blade surfaces have characteristics in common with those of some of the Fe pnictides,[27,28] all of which have this same trilayer. The similarity is that the top view of the fan blades (if one ignores the diamond-shaped cutout at the intersection, centered at Γ) appears to show intersecting FSs, neither of which has the square symmetry of the lattice.

Such occurrence of intersecting FSs, each with lower symmetry than the lattice, has been analyzed for LaFeAsO (a "1111" compound) by Yaresko *et al.*[29] A symmetry of the Fe_2As_2 (also Al_2Si_2) substructure is a non-primitive translation connecting Fe atoms (respectively, Al atoms) followed by z-reflection. This operation leads to symmetries that allow $k_z = 0$ bands to be unfolded into a larger Brillouin zone (that is, a "smaller unit cell" having only one Fe atom) which *un*folds the band structure and the intersecting FSs. The NaAlSi FSs appear to have this similar crossing (albeit interrupted by the free-electron bands), and the highly anisotropic dispersion is due to distinct (but symmetry-related) hopping along each of the crystal axes. In this respect NaAlSi may clarify the electronic structure of the pnictides: by analogy, there are separate bands that disperse more strongly along the $(1,1)$ direction or the $(1,-1)$ direction, and give rise to the intersecting, symmetry-related surfaces. In NaAlSi the bands are much more anisotropic in the plane (approaching one-dimensional), making such character much clearer. A difference that complicates the analogy is that in the pnictides the bands near ε_F are derived from the Fe atoms, which comprise the center layer of the trilayer, whereas in NaAlSi the bands under discussion are derived from the Si atoms, which comprise the two outer layers.

D. Wannier functions

Pictured in Fig. 5 are symmetry-projected Wannier functions (WFs) projected onto Si $3p$ orbitals. The extension of the WFs shows considerable involvement from nearby Al and Si atoms, and in addition have some density extending into the Na layers. The p_x WF consists of an atomic p_x function, with its density shifted downward by the bonding

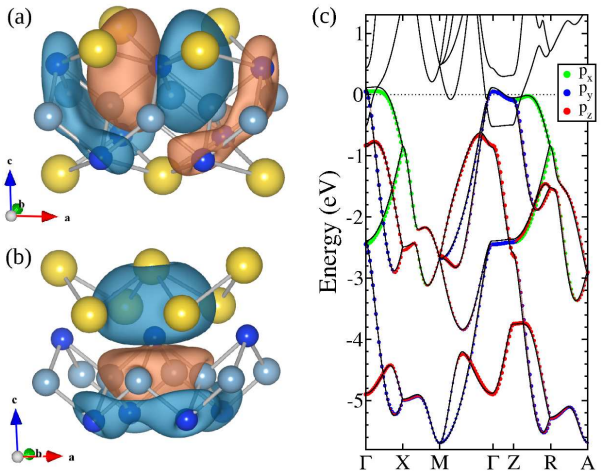

FIG. 5: (Color online.) Isosurface of the WFs for (a) Si $3p_x$ and (b) Si $3p_z$. Na atoms are large and yellow (light) colored, Si atoms are small and blue (dark) colored. The two colors of the isosurface represent different signs. (c) The tight-binding fatbands band structure described in the text for the WFs, compared to the DFT band structure (black lines).

		p_x	p_y	p_z
a	p_x	761		60
	p_y		-62	60
	p_z	60	60	-40
2a	p_x	128		27
b	p_x	361	300	360
	p_y	300	361	360
	p_z	360	360	360
b*	p_x	12	5	50
	p_y	5	12	50
	p_z	50	50	185

TABLE I: Selected hopping integrals in meV for the Si $3p$ WFs along the vectors $\mathbf{a} = (a, 0, 0)$ (hopping within a Si layer), $\mathbf{b} = (a/2, a/2, d)$ (hopping across an Al layer), and $\mathbf{b}^* = (a/2, a/2, c-d)$ (hopping across a Na layer). d is the distance in the z direction between Si atoms above and below Al planes.

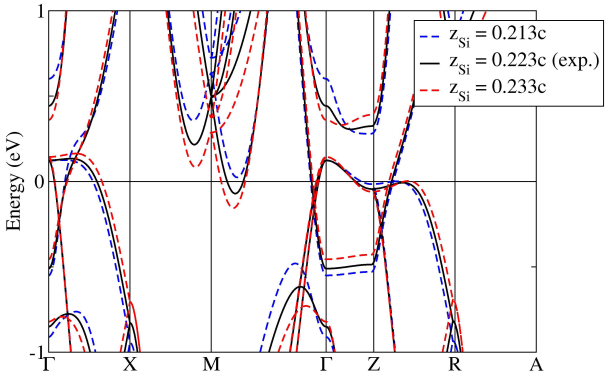

FIG. 6: (Color online.) Comparison of band structures near ε_F for different z_{Si} values.

contribution of Al sp^3 hybrid orbitals. Beyond the p_x lobes the nearest Si atoms form a bonding lobe that connects to the "small" side of the Al sp^3 function. The large p_x lobes and the extra contribution from nearby Si atoms are responsible for the largest hopping amplitudes shown in Table I, although there is some phase cancellation between the p_x lobe and the lobe lying beyond the nodal surface.

The p_z WF has one lobe extended well into the Na layer; this is responsible for the largest hoppings along $\mathbf{b}^*$ in Table I, and they create the large dispersion in the p_z bands seen in Fig. 5(c). Again, the Al atoms contribute with an sp hybrid orbital, although it appears to be more sp^2-like than sp^3-like. There is also a "ring" structure below the Al layer, where an sp hybrid orbital from the Si atoms forms a bonding combination, but it is antibonding with the p_z function on the central Si. The largest contribution to near-neighbor hopping in the Al-Si plane between p_z and p_x or p_z is most likely due to this ring structure, as the p lobes are confined to the inside of a square of near-neighbor Al atoms, which are only edge sharing with the nearest Si atoms along $\mathbf{b}$ vectors. This is the likely reason that all the hoppings along $\mathbf{b}$ are approximately of the same magnitude. The dispersion which creates the FSs along Γ-Z (seen in Fig. 4) is composed only of the p_x and p_y WFs. This is not caused by the large hoppings, but by smaller hoppings along $\mathbf{b}^*$ between p_x and p_y WFs. Without these small hoppings, the band just above ε_F is dispersionless along Γ-Z.

IV. RESPONSE TO CHANGES

A. Electron-ion coupling

A deformation potential $\mathcal{D}$ is the shift in an energy band with respect to sublattice atomic displacement. One can freeze in phonon modes to calculate deformation potentials, which at the FS are directly connected to electron-phonon matrix elements.[30]

Moving the Si atoms in the z direction by ±1% of the experimental parameter, such that the tetrahedra surrounding the Al atoms stretch or flatten (while remaining centered on Al), gives an average deformation potential of ∼0.8 eV/Å over five band positions near the Fermi level. The largest shift is for the ellipsoidal electron pockets, with $\mathcal{D} \sim 1.2$ eV/Å. These ellipsoids disappear when the Si atoms are displaced toward the Al plane (see Fig. 6).

Flattening the Na bilayer, so as to remove the buckling of the Na atoms, requires a (very large) 12% change in the z component of the Na atoms. We chose such a large displacement because we do not expect a substantial deformation potential for Na movement. Even this large displacement does not alter very much the valence bands, as expected, and the hole FSs remain virtually unchanged. The conduction bands at the Fermi level however shift appreciably, resulting in a modulation of the electron ellipsoids along (1,1) near M. In addition, the accidental four-band near-degeneracy that is 0.5 eV above ε_F at M splits the two separate doubly-degenerate states, opening up a gap of ∼0.7 eV, which is equivalent to a deformation potential of ∼0.8 eV/Å (but the bands are not at ε_F).

B. Magnetic susceptibility

The magnetic spin susceptibility χ is given by

$$\chi = \frac{\partial M}{\partial H} = (\partial^2 E/\partial M^2)^{-1}.$$

Fixed-spin-moment calculations were conducted to produce an energy-vs.-moment $E(M)$ curve, resulting in a susceptibility of $\chi = 2.93\ \mu_B^2\ \mathrm{eV}^{-1}$, or 3.76×10^{-6} emu/mol. This is the exchange-enhanced susceptibility in the Stoner theory, and can be written as

$$\chi = S\chi_0 \equiv \frac{\chi_0}{1 - IN(\varepsilon_F)},$$

where $S \equiv \chi/\chi_0$ is the Stoner enhancement factor, I is the Stoner parameter, and the bare Pauli susceptibility χ_0 is equal to $\mu_B^2 N(\varepsilon_F)$. Janak has shown how to calculate I within density functional theory,[31] which must be equivalent (within a minor approximation he used) to our approach of using fixed-spin-moment calculations.

With our calculated values we obtain $S = 2.75$, which translates to $I = 0.60$ eV. Some interpretation of this value of Stoner I should be noted. First, ε_F falls where most of the states are Si-derived, so for simplicity we neglect Al (and Na, which is ionized). Second, we note that there are two Si atoms in the primitive cell. Thus to get an "atomic value" of I_{Si}, we should use a value of $N(\varepsilon_F)/2$ per Si atom. The result then is very roughly $I_{Si} \sim 1$ eV. This value can be compared to the atomic value for Al (next to Si in the periodic table) in the elemental metal, which is $I_{Al} = 0.6$ eV.[31] It seems, therefore, that Si in NaAlSi is considerably more "magnetically inclined" than is Al in aluminum. However, the Stoner enhancement overall is not large, indicating relatively modest magnetic enhancement and rather conventional magnitude of magnetic interactions.

C. Comparison to NaAlGe

Isostructural and isovalent NaAlGe is not superconducting (above 1.6 K, at least), so it should be instructive to compare its electronic structure to that of NaAlSi. Using its experimental lattice parameters,[23] we have calculated the band structure of NaAlGe, and compared it with that of NaAlSi on a rather fine scale in Fig. 7. The band structures are very similar, the one difference being that the band along Γ-M near M does not cross ε_F in NaAlGe. The free-electron band is also identical.

Supposing the tiny bit of FS along Γ-M cannot account for the difference in superconducting behaviors, the factors relevant for electron-phonon coupling will be the difference in mass (Ge is more than twice as heavy as Si) and the difference in electronic character, which can affect force constants and electron-phonon matrix elements. A real possibility is that the pairing mechanism is electronic rather than phononic. In three dimensions purely electronic pairing mechanisms have been attracting serious study (by Sham and collaborators[32,33] for example), but 2D semimetals introduce new features that deserve detailed study.

Another possibility is that these pockets are important, and that superconductivity arises from an enhancement of electron-phonon coupling in these tiny electron pockets from low frequency electronic response, either interband transitions or plasma oscillations, or both. A model in which the electronic response of a 2D electronic superlattice plays a central role in the mechanism has been previously studied[34,35] using a model of parallel conducting sheets separated by a dielectric spacer. This model may be useful as a starting point for understanding NaAlSi.

V. DISCUSSION

The classes of materials that contain relatively high temperature superconductors[36] continues to expand. Superconductors derived from doped 2D semiconductors pose many of the most interesting issues in superconductivity today. The cuprates and the Fe-pnictides (and -chalcogenides) are strongly magnetic, and comprise one end of the spectrum (though they are themselves quite different). On the other end lie those with little, perhaps negligible, magnetism: electron-doped ZrNCl and HfNCl, and electron-doped TiNCl. There are several other, lower-T_c systems, whose behavior seems different still (hydrated Na_xCoO_2, $Li_{1-x}NbO_2$, and several

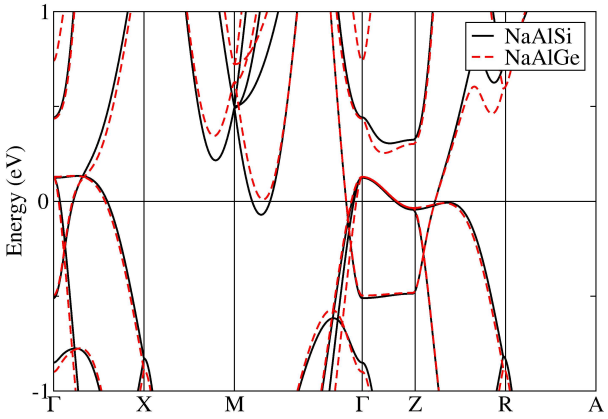

FIG. 7: (Color online.) Blowup of the band structures of NaAlSi and NaAlGe near ε_F.

transition-metal disulfides and diselenides).

A common feature of most of these systems is that they are 2D and have a small, but not tiny, concentration of charge carriers, often in the range of 0.05–0.15 carriers per unit cell. These materials also have ionic character. NaAlSi differs in that it has *sp* carriers—the others have carriers in *d* bands—and is self-doped, a compensated semimetal. We suggest that a useful view of NaAlSi is that it be regarded as arising from an underlying ionic semiconductor, but that it has a small *negative* gap rather than a true gap. Without the overlap of the valence and conduction bands, it would be a 2D, ionic, and somewhat covalent semiconductor like the aforementioned nitridochloride compounds, which superconduct in the 15–25 K range. Comparing the characteristics of these two classes of superconductors should further the understanding of 2D superconductivity.

VI. ACKNOWLEDGMENTS

This work was supported by DOE grant DE-FG02-04ER46111, the Strategic Sciences Academic Alliance Program under grant DE-FG03-03NA00071, and by DOE SciDAC Grant No. DE-FC02-06ER25794.

[1] Y. Kamihara, T. Watanabe, M. Hirano, and H. Hosono, J. Am Chem. Soc. **130**, 3296 (2008).
[2] S. Yamanaka, H. Kawaji, K. Hotehama, and M. Ohashi, Adv. Mater. **8**, 771 (1996).
[3] S. Shamoto, T. Kato, Y. Ono, Y. Miyazaki, K. Ohoyama, M. Ohashi, Y. Yamaguchi, and T. Kajitani, Physica C **306**, 7 (1998).
[4] S. Yamanaka, K. Hotehama, and H. Kawaji, Nature **392**, 580 (1998).
[5] S. Shamoto, K. Iizawa, M. Yamada, K. Ohoyama, Y. Yamaguchi, and T. Kajitani, J. Phys. Chem. Solids **60**, 1431 (1999).
[6] S. Yamanaka, T. Yasunaga, K. Yamaguchi, and M. Tagawa, J. Mater. Chem. **19**, 2573 (2009).
[7] S. Kuroiwa, H. Kawashima, H. Kinoshita, H. Okabe, and J. Akimitsu, Physica C **466**, 11 (2007).
[8] E. Bustarret, C. Marcenat, P. Achatz, J. Kačmarčik, F. Lévy, A. Huxley, L. Ortéga, E. Bourgeois, X. Blase, D. Débarre, and J. Boulmer, Nature **444**, 465 (2006).
[9] L. F. Mattheiss, E. M. Gyorgy, and D. W. Johnson, Jr., Phys. Rev. B **37**, 3745 (1988).
[10] S. Jin, T. H. Tiefel, R. C. Sherwood, A. P. Ramirez, E. M. Gyorgy, G. W. Kammlott, and R. A. Fastnacht, Appl. Phys. Lett. **53**, 1116 (1988).
[11] E. A. Ekimov, V. A. Sidorov, E. D. Bauer, N. N. Mel'nik, N. J. Curro, J. D. Thompson, and S. M. Stishov, Nature **428**, 542 (2004).
[12] H. Rosner, A. Kitaigorodsky, and W. E. Pickett, Phys. Rev. Lett. **88**, 127001 (2002).
[13] H. Sagayama, Y. Wakabayashi, H. Sawa, T. Kamiyama, A. Hoshikawa, S. Harjo, K. Uozato, A. K. Ghosh, M. Tokunaga, and T. Tamegai, J. Phys. Soc. Jpn. **75**, 043713 (2006).
[14] S. Kuroiwa, H. Sagayama, T. Kakiuchi, H. Sawa, Y. Noda, and J. Akimitsu, Phys. Rev. B **74**, 014517 (2006).
[15] I. R. Shein, N. I. Medvedeva, and A. L. Ivanovskii, J. Phys.: Condens. Matter **15**, L541 (2003).
[16] G. Q. Huang, L. F. Chen, M. Liu, and D. Y. Xing, Phys. Rev. B **69**, 064509 (2004).
[17] I. I. Mazin and D. A. Papaconstantopoulos, Phys. Rev. B **69**, 180512 (2004).
[18] M. Giantomassi, L. Boeri, and G. B. Bachelet, Phys. Rev. B **72**, 224512 (2005).
[19] R. Heid, K. -P.Bohnen, B. Renker, P. Adelmann, T. Wolf, D. Ernst, and H. Schober, J. Low Temp. Phys. **147**, 375 (2007).
[20] S. Kuroiwa, A. Q. R. Baron, T. Muranaka, R. Heid, K. -P. Bohnen, and J. Akimitsu, Phys. Rev. B **77**, 140503(R) (2008).
[21] K. Koepernik and H. Eschrig, Phys. Rev. B **59**, 1743 (1999).
[22] J. P. Perdew and Y. Wang, Phys. Rev. B **45**, 13244 (1992).
[23] W. Westerhaus and H. U. Schuster, Z. Naturforsch. **34b**, 352 (1979).
[24] K. Momma and F. Izumi, J. Appl. Cryst. **41**, 653 (2008).
[25] A. B. Kyker and W. E. Pickett, Phys. REv. B **71**, 224517 (2005).
[26] H. Rosner, R. Weht, M. D. Johannes, W. E. Pickett, and E. Tosatti, Phys. Rev. Lett. **88**, 027001 (2002).
[27] D. J. Singh, Phys. Rev. B **78**, 094511 (2008).
[28] I. I. Mazin, D. J. Singh, M. D. Johannes, and M. H. Du, Phys. Rev. Lett **101**, 057003 (2008).
[29] A. N. Yaresko, G.-Q. Liu, V. N. Antonov, and O. K. Andersen, Phys. Rev. B **79**, 144421 (2009).
[30] F. S. Khan and P. B. Allen, Phys. Rev. Lett. **29**, 3341 (1984).
[31] J. F. Janak, Phys. Rev. B **16**, 255 (1977).
[32] H. Rietschel and L. J. Sham, Phys. Rev. B **28**, 5100 (1983).
[33] M. Grabowski and L. J. Sham, Phys. Rev. B **29**, 6132 (1984).
[34] A. Bill, H. Morawitz, and V. Z. Kresin, Phys. Rev. B **66**, 100501 (2002).
[35] A. Bill, H. Morawitz, and V. Z. Kresin, Phys. Rev. B **68**, 144519 (2003).
[36] W. E. Pickett, Physica B **296**, 112 (2001).